Clin Oncol Cancer Res (2009) 6: 256-262
DOI 10.1007/s11805-009-0256-y

Biodistribution and Anti-tumor Activities of the ^{131}I-labeled Rituximab in Nude Mice Bearing Human Burkitt's lymphoma

Qiang Zuo
Aimin Li
Xiao Yan
Rongcheng Luo

Cancer Center, Nanfang Hospital, the Southern Medical University, Guangzhou 510515, Guangdong Province, China.

Correspondence to: Rongcheng Luo
Tel: 86-20-6164 1651
E-mail: nfyywbb@126.com

Received June 8, 2009; accepted July 28, 2009.

E-mail: 2008cocr@gmail.com
Tel (Fax): 86-22-2352 2919

OBJECTIVE To explore the biodistribution and anti-tumor activity of ^{131}I labeled rituximab injected intratumorally or intraperitoneally in vivo in nude mice bearing Raji human Burkitt's lymphoma xenografts.

METHODS The rituximab and the mouse IgG were labeled with Na^{131}I using the IODO-GEN method. BALB/C nude mice were *xenografted* with ^{131}I-Rituximab or ^{131}I-IgG and killed on the 1st, 3rd, 7th, and 15th day after injection. The tumor/non-tumor ratio (T/NT) and the dose injected in each gram of the tissue (%ID/g) from 12 organs or tissues of interest, e.g. tumor, blood, were calculated. The long and short axes of each tumor were measured by calipers at 2-3-day intervals after treatment, and the growth inhibition of the tumor was calculated using the MIRD formula.

RESULTS When comparing intraperitoneal injection (IP) and intratumoral injection (IT) of ^{131}I-IgG, intratumoral injection of ^{131}I-rituximab produced a significantly higher tumor/non-tumor ratio in all tissues and organs of interest on the 1st, 3rd, and 7th day, respectively ($P < 0.05$). The %ID/g of tumor was 1.4-1.7-fold and 1.5-3.7-fold in the IP and IgG IT groups, respectively, but the %ID/g of non-tumors was significantly lower in the IP group and IgG IT group. Similarly, the tumor growth was greatly inhibited by intratumoral injection of the ^{131}I-rituximab, whereas it was less inhibited by other forms of the treatment ($P < 0.05$). However ^{131}I-rituximab injected intratumorally inhibited tumor growth in a dose-dependent manner. The inhibition rate was less with a low dose (75 μCi) and greater with a high dose (150 μCi), yet the difference was not significant ($P > 0.05$).

CONCLUSION Tumors can absorb the highest amount of the radiolabelled antibodies, and the tumor/non-tumor ratios in the group with intratumoral injection of the ^{131}I-rituximab resulted in the optimal anti-tumor activity.

KEY WORDS: Iodine-131, anti-CD20 monoclonal antibody, non-Hodgkin's lymphoma (NHL), intratumoral injection, radioimmunotherapy.

Introduction

^{131}I has been used primarily as radionuclide for either radioimmunotherapy or imaging due to its advantageous characteristics of high availability, low cost, and ease of labeling. The CD20 antigen is specifically expressed on 90%-95% of B lymphoma cells[1]. In this experiment, we studied the biodistribution and antitumor activities of Rituximab with ^{131}I labeled CD20 monoclonal antibody injected intratumorally or intraperitoneally in vivo in nude mice bearing Raji

human Burkitt's lymphoma xenografts.

Materials and Methods

Materials

Rituximab chimeric anti-CD20 monoclonal antibody was supplied by Roche Pharma (Schweiz) Ltd, mouse IgG was supplied by SIGMA, $Na^{131}I$ solution was purchased from Chengdu Gaotong Isotope Co., and Raji cell lines (human Burkitt's lymphoma) was purchased from Shanghai Institute of Biochemistry and Cell Biology, Chinese Academy of Science. The level of CD20 expression was determined using flow cytometry.

Antibody labeling protocols and assay of the label activity

The Rituximab and the mouse IgG were labeled with $Na^{131}I$ using IODO-GEN methods, with the ratio of antibody weight (mg) to ^{131}I radioactivity (mCi) being 1:10. The labeled yield and radiochemical purity were measured using paper chromatography, and the immune competence was measured using the method of excessive antigen binding of tumor.

Grouping of experimental animal

BALB/C nude mice were provided by the Institute of Laboratory Animals of the Southern Medical University. The experimental animal model was established by subcutaneously injecting suspensions of $6\text{-}7\times10^6$ Raji cells in exponential growth phase into the right buttock of the BALB/C nude mice. The nude mice whose maximum diameter of the tumor ranged from 0.5-1.5 cm were selected for use in subsequent experiments. They were randomized respectively into 4 and 6 groups as shown in Table 1 and Table 2. The set of 4 groups was utilized for the biodistrubution experiment in vivo, and the set of 6 groups for the radioimmunotherapy experiment. The control cells were MCF-7 cells and A549 cells.

The dynamic biodistribution of ^{131}I-labeled Rituximab in vivo in the nude mice

The ^{131}I-Rituximab and ^{131}I-IgG were administrated to the nude mice following the predetermined protocols. The mice were imaged using single photon emission computed tomography (SPECT, or less commonly used SPET) on the 1st, 3rd, 7th and 15th day after injection and then killed to harvest the organs or tissues of interest, including blood, tumor, liver, spleen, kidney, heart, lung, stomach, large intestine, small intestine, contralateral leg muscles, and femur. Radioactivity (cpm) was measured using a calibrator. The special radioactivity of the tissue (cpm/g) and the injected dose per gram of tissue (%ID/g) were calculated according to the following formula:

%ID/g = special radioactivity of tissue (cpm/g)/radioactivity of injected labels (cpm)

Table 1. Grouping of nude mice bearing tumor.

Group	Injected marked-drugs	Injection approach	Radioactivity (μCi)	Volume injected (μl)
1	^{131}I-IgG	IT	50	38
2	^{131}I + rituximab	IT	50	11
3	^{131}I-rituximab	IP	50	11
4	^{131}I-rituximab	IT	50	11

IT, intratumor injection; IP, intraperitoneal injection; ^{131}I + rituximab, mixing of ^{131}I and rituximab.

Cumulative absorbed dose

The injected dose per gram tissue values of the labeled antibodies in nude mice were used to calculate the cumulative absorbed dose in tumor tissue according to the formula recommended by the MIRD Committee[2]. Curve fitting was performed for each group, and the area under the curve was determined using the integration method, which was added with 0.5 μCi (1% injection volume) to obtain the value of A_h/m_k (μCi·h/g). This was then applied to the following formula to calculate the cumulative absorbed dose (Gy):

$$D_k = A_h/m_k[\sum np \triangle np \varphi np(r_k \leftarrow\rightarrow r_h)+\sum p \triangle p \varphi p(r_k \leftarrow\rightarrow r_h)]$$

D_k is the absorbed dose of target organ k (rad). A_h is the cumulative activity of source organs (μCi·h). m_k is the weight of target organ k (g). np represents non-penetrating radiation. p represents penetrating radiation. $\triangle$ represents the average energy radiation per cumulative activity (g·rad/μCi·h). φ is the absorption coefficient. $r_k \leftarrow\rightarrow r_h$ means that the target organs are the same as the

Table 2. Grouping and treatment protocols.

Group	Treatment protocol	Injection approach	Radioactivity MBq (μCi)	Volume injected (μl)	Types of tumor
1	0.05 MPB (nontreatment)	IT	0	22	Raji
2	^{131}I-NMIgG	IT	5.55 (150)	22	Raji
3	^{131}I-rituximab	IP	5.55 (150)	22	Raji
4	^{131}I-rituximab	IT	2.78 (75)	22	Raji
5	^{131}I-rituximab	IT	5.55 (150)	22	Raji
6	^{131}I-rituximab	IT	5.55 (150)	22	Control

source organs. $\sum np \triangle np \varphi np(r_k \leftarrow\!\!\rightarrow r_h) + \sum p \triangle p \varphi p(r_k \leftarrow\!\!\rightarrow r_h)$ is the absorbed dose of unit cumulative radioactivity in unit time for a given radionuclide and organ. In our experiment, ^{131}I was 0.421 g·rad/μCi·h.

Observation of therapeutic effects

The nude mice were evaluated for tumor growth before treatment and each day after treatment for 39 days. The long and short axes of the tumors were measured with calipers, and the formula of tumor size (short axis^2 × long axis)/2, was applied to calculate the tumor size precisely. The growth inhibition of the tumor was calculated by the following formula:

Growth inhibition rate of tumor (%) = 100 − (mean tumor size of the treatment group/mean tumor size of the non-treatment group) × 100

Statistical analysis

Data were performed with one-way analysis of variance (ANOVA) using SPSS 10.0 statistical software. A value of $P < 0.05$ was considered statistically significant.

Results

The labeling yield, radiochemical purity, and immunoreactivity of the ^{131}I-Rituximab and ^{131}I-IgG

The labeling yield, radiochemical purity, and immunoreactivity of the ^{131}I-Rituximab and ^{131}I-IgG are shown in Table 3.

The T/NT ratio after injection of the ^{131}I-Rituximab and ^{131}I-IgG

As shown in Table 4, the T/NT ratio in the blood of ^{131}I-Rituximab IT group was 7.4, 12.3, and 2.4, respectively on the 1st, 3rd, and 7th day after injection, which was significantly higher than in the IP group and in the ^{131}I-IgG IT group ($P < 0.05$). Similarly, the T/NT ratios in the other tissues and organs were high in the ^{131}I-Rituximab IT group. However, there was no significant difference in T/NT ratio between ^{131}I-Rituximab IT and IP groups on the 15th day after injection ($P > 0.05$).

The %ID/g after injection of the ^{131}I-Rituximab and ^{131}I-IgG

Intratumoral injection of ^{131}I-Rituximab produced a dramatically higher %ID/g in tumors on the day of each injection in comparison to intraperitoneal injection (1.4-17-fold) or to intratumoral injection of ^{131}I-IgG (1.7-3.7-fold), respectively, whereas the opposite result was noticed in non-tumors, aside from a few instances, i.e. the %ID/g in heart tissue measured on the 15th day after injection, and a lower %ID/g in non-tumors in the ^{131}I-Rituximab IT group. For ^{131}I-IgG treatment protocols, the %ID/g in tumors was higher in the ^{131}I-IgG IT group than that in the ^{131}I-Rituximab IP group on the 1st day after injection (42.2 *vs.* 5.1, $P < 0.05$). The difference, as shown in Table 5, declined with prolonged time, and by the 3rd day after injection, there were no differences between the 2 groups ($P > 0.05$). For the mice receiving intratumoral injection of the ^{131}I and rituximab

Table 3. Labeling parameters of the ^{131}I-Rituximab and ^{131}I-IgG.

Label	Labeling yield (%)	Radiochemical purity (%)	Cell binding rate (%)	Special radioactivity	
				Volume [MBq (mCi)/ml]	Weight [MBq (mCi)/mg]
^{131}I-rituximab	72.4	95.2	28.5	170 (4.6)	244 (6.6)
^{131}I-IgG	64.0	95.9	6.37	48 (1.3)	323 (8.7)

Table 4. T/NT ratio of different radiolabeled antibodies in different sites of injection after various days.

Organ or tissue	T/NT ratio										
	1 d			3 d			7 d			15 d	
	IgG	IT	IP	IgG	IT	IP	IgG	IT	IP	IT	IP
Blood	4.0	7.4	0.3	0.8	12.3	0.6	1.1	2.4	0.8	1.9	1.3
Muscle	39.3	125.3	3.1	9.8	153.4	4.8	14.4	24.4	8.7	17.8	12.9
Heart	19.4	30.1	1.6	4.6	62.6	2.4	5.9	10.3	3.3	8.7	6.1
Liver	10.2	23.3	1.2	2.7	78.1	2.6	4.2	9.5	3.2	9.6	5.8
Spleen	10.9	29.0	1.3	2.4	68.9	2.9	3.2	8.6	3.5	9.9	5.4
Lung	6.8	14.8	0.8	2.4	32.8	1.5	3.1	5.3	1.7	4.3	2.7
Kidney	11.9	25.5	1.0	3.1	55.8	2.2	5.3	8.5	3.1	7.8	4.8
Stomach	29.4	46.5	2.1	6.1	97.1	4.3	10.2	17.5	5.6	14.4	7.6
Small intestine	20.5	35.5	1.9	5.2	88.9	4.0	7.0	14.0	5.2	15.2	10.3
Large intestine	18.6	36.1	1.9	5.2	107.6	3.8	6.8	13.9	5.1	13.2	7.8
Bone	22.7	63.1	2.6	5.9	117.8	3.8	9.3	21.2	7.1	16.0	8.4

Table 5. The %ID/g of different radiolabeled antibodies in different sites of injection after various days.

Organ or tissue	%ID/g value										
	1 d			3 d			7 d			15 d	
	IgG	IT	IP	IgG	IT	IP	IgG	IT	IP	IT	IP
Tumor	42.2	84.0	5.1	8.9	33.1	7.7	6.2	10.6	5.5	2.7	1.9
Blood	11.3	10.6	17.0	11.7	4.8	13.7	6.1	5.0	7.3	1.7	2.1
Muscle	1.6	0.8	1.7	0.9	0.5	1.7	0.5	0.5	0.6	1.0	0.2
Heart	2.4	2.6	3.5	1.9	1.2	3.3	1.1	1.1	1.4	0.4	0.5
Liver	4.5	4.5	4.3	3.1	1.1	3.1	1.5	1.1	1.4	0.3	0.5
Spleen	4.3	4.1	4.3	3.8	0.9	3.2	2.3	1.3	1.7	0.4	0.5
Lung	10.5	5.5	6.9	3.9	2.3	5.5	2.2	2.2	3.2	0.7	1.0
Kidney	3.8	3.3	4.5	2.8	1.2	3.6	1.3	1.3	2.0	0.4	0.6
Stomach	1.4	1.9	2.5	1.4	0.7	1.9	0.6	0.7	1.1	0.2	0.3
Small intestine	3.7	2.3	3.0	1.8	0.8	2.1	0.9	0.8	1.2	0.2	0.3
Large intestine	2.8	2.3	2.9	1.8	0.9	2.1	0.9	0.9	1.5	0.3	0.3
Bone	3.3	1.4	2.2	1.5	0.6	2.3	0.7	0.6	0.9	0.2	0.3

mixture, the %ID/g in tumors was reduced from 192.4 at the moment of injection to 0.6 at 24 h after injection.

Cumulative absorbed dose

As shown in Table 6, the cumulative absorbed dose in the ^{131}I-Rituximab IT group was higher than that in the other groups at each time point of detection. Specifically, it was 12.6-fold and 2.1-fold in the IP group and in the ^{131}I-IgG IT group on the 3rd day after injection, 6.0-fold and 2.5-fold on the 7th day after injection, 7.0-fold and 1.5-fold on the 15th day after injection, respectively.

Table 6. Cumulative absorption in tumor of each group on different days after injection.

Group	Cumulate absorption in tumor on different days after injection (Gy)		
	3 d	7 d	15 d
^{131}I-IgG (IT)	5.15	5.65	13.99
^{131}I-rituximab (IT)	10.83	13.90	21.65
^{131}I-rituximab (IT)	0.86	2.32	3.09
^{131}I-rituximab (IT)	0.07	0.10	0.46

Radioimmunoimaging

Radioimmunoimaging was performed on the 1st, 3rd, and 7th day after injection. As shown in Fig.1, the tumors were clearly visible in the ^{131}I-Rituximab IT group, but invisible in IP group throughout the study. For the ^{131}I-IgG IT group, tumors were clearly visible on the 1st day after injection, which, however, became blurred on the 3rd day after injection and indistinguishable on the 7th day after injection. There was no recognized tumor observed in ^{131}I + rituximab IT group even on the 1st day after injection.

Changes in tumor size as a result of the function of treatment protocols

The changes in tumor size are shown in Table 7. In general, tumors increased in size shortly after the initiation of radioimmunotherapy, irrespective of the treatment protocol used. Specifically, tumors grew at a relatively slow speed in groups 2-5 after the initiation of radioimmunotherapy, as shown in Table 7. The tumors became gradually smaller following the 14th day after injection in groups 3-5. Similar behavior was seen in group 2 during the 10th-24th days after injection, but unfortunately, the tumors started to increase in size following the 26th day after injection in group 2. In contrast, tumors in group 1 and 6 grew rapidly at first, while those in group 1 became gradually smaller upon the 19th day after injection, and those in group 6 grew progressively throughout the experiment. These results suggested that both intratumoral and intraperitoneal injection of the ^{131}I-Rituximab had certain inhibitive effects on the growth of Raji lymphoma, however, the former was superior to the latter in therapeutic effects. The IT and IP injection of the ^{131}I-Rituximab had no inhibitive effects on MCF7 or A549 cell tumors, and although intratumoral injection of ^{131}I-IgG inhibited the growth of Raji lymphoma to a some extent, the effects were transient.

Comparison of inhibition rate of tumor

Both groups of ^{131}I-Rituximab and ^{131}I-IgG, injected intratumorally or intraperitoneally, exhibited a greater inhibition rate of tumor growth than the control group ($P < 0.05$). Intraperitoneal injection of the ^{131}I-Rituximab resulted in a lower tumor inhibition rate than the intratumoral injection of ^{131}I-Rituximab. This difference was statistically insignificant when compared with IT

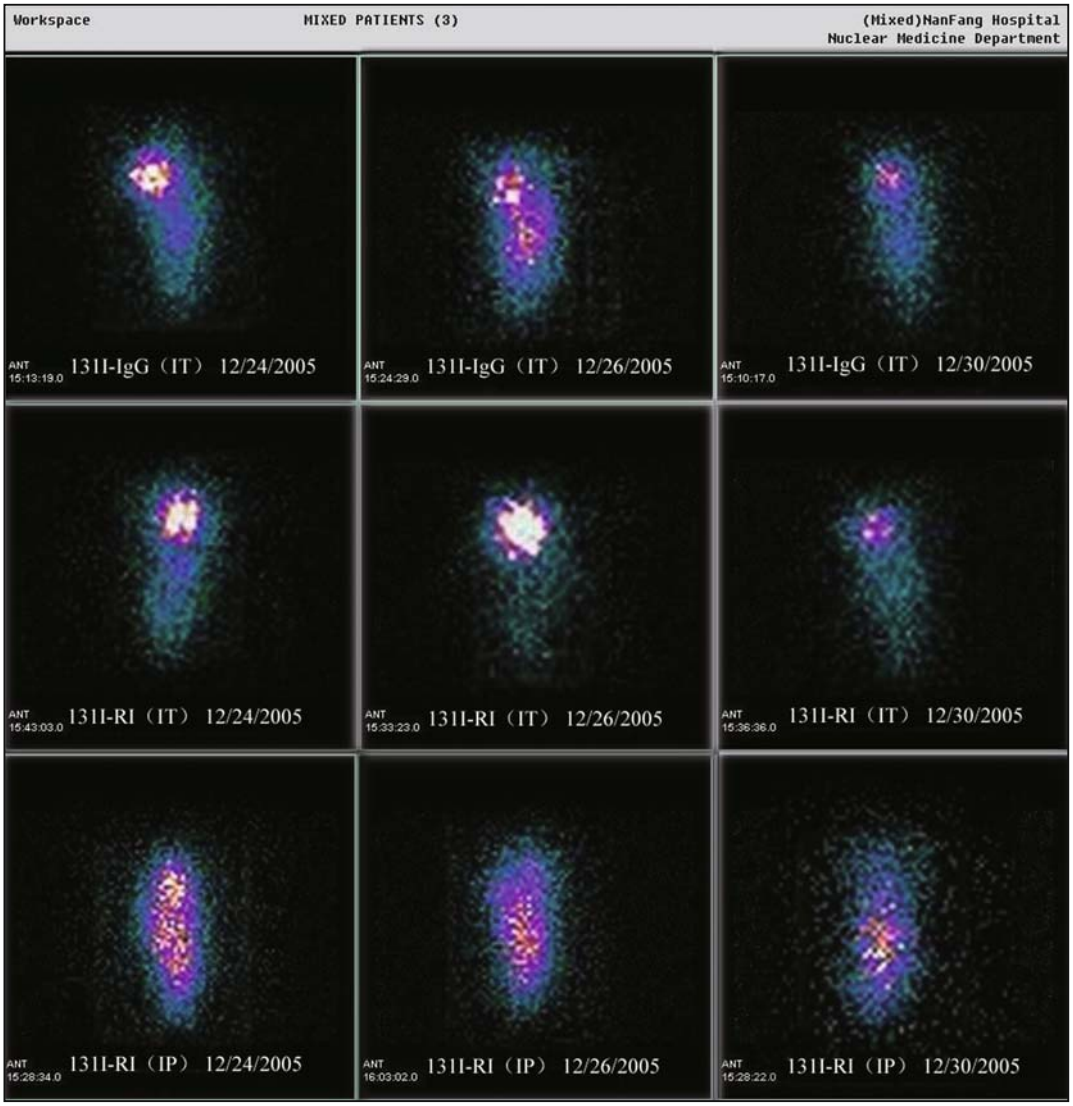

Fig.1. Radioimmunoimage of nude mice xenografted with tumor after injection with radiolabeled antibody.

Table 7. The average volume of the tumor in each group on different days after injection.

Day	Tumor volume ($\bar{x} \pm s$)					
	Group 1	Group 2	Group 3	Group 4	Group 5	Group 6
1	1	1	1	1	1	1
3	1.93 ± 2.28	1.07 ± 0.30	1.61 ± 0.58	1.33 ± 0.30	1.31 ± 0.29	1.28 ± 0.24
5	2.62 ± 3.63	1.16 ± 0.16	2.10 ± 1.21	1.43 ± 0.37	1.28 ± 0.40	1.40 ± 0.38
7	2.42 ± 3.43	1.11 ± 0.40	1.86 ± 1.16	1.47 ± 0.54	1.05 ± 0.33	1.44 ± 0.29
10	2.29 ± 3.00	0.85 ± 0.40	1.60 ± 1.31	1.46 ± 0.68	1.25 ± 1.05	1.40 ± 0.46
12	2.29 ± 2.86	0.95 ± 0.74	1.87 ± 1.75	1.59 ± 0.85	1.26 ± 1.18	1.82 ± 0.80
14	2.33 ± 2.92	0.84 ± 0.80	1.74 ± 2.04	1.65 ± 0.90	1.06 ± 1.13	2.02 ± 0.97
17	1.98 ± 2.24	0.98 ± 1.28	1.65 ± 2.37	1.43 ± 1.02	0.98 ± 1.26	2.04 ± 1.25
19	1.80 ± 2.12	1.16 ± 1.78	1.59 ± 2.49	1.41 ± 1.13	0.91 ± 1.39	2.12 ± 1.35
21	1.54 ± 1.78	0.86 ± 1.30	1.42 ± 2.21	1.24 ± 1.13	0.58 ± 0.84	1.90 ± 1.37
24	1.41 ± 1.59	0.83 ± 1.41	1.39 ± 2.25	1.14 ± 1.07	0.52 ± 0.80	2.17 ± 1.74
26	1.18 ± 1.18	1.20 ± 2.12	1.33 ± 2.29	1.27 ± 1.23	0.53 ± 0.84	2.29 ± 1.83
28	1.04 ± 1.04	1.27 ± 2.26	1.32 ± 2.31	1.27 ± 1.25	0.49 ± 0.80	2.44 ± 2.05
31	1.01 ± 1.06	1.45 ± 2.74	1.25 ± 2.27	1.10 ± 1.10	0.34 ± 0.54	2.62 ± 2.19
33	1.02 ± 1.14	1.43 ± 2.68	1.14 ± 2.07	0.97 ± 0.96	0.39 ± 0.63	2.79 ± 2.36

75 μCi group (P = 0.616), but statistically significant when compared with IT 150 μCi group (P = 0.047). The inhibition rate of the tumor was higher in the ^{131}I-Rituximab IT 150 μCi group than in the ^{131}I-Rituximab IT 75 μCi group, but the difference was not significant (P = 0.134). For the ^{131}I-IgG IT group, the inhibition rate of the tumor was lower in the ^{131}I-IgG IT group than in the ^{131}I-Rituximab IT group. When compared with the ^{131}I-Rituximab IT 75 μCi group, the difference was statistically insignificant (P = 0.463) but was statistically significant when compared with the IT 150 μCi group (P = 0.012). The detailed results are presented in Table 8.

Table 8. The inhibition rate of tumor growth in each group after injection (%).

Group	Tumor inhibition rate
^{131}I-IgG (IT, 150 μCi)	16.81 ± 48.77**
^{131}I-rituximab (IT, 75 μCi)	17.91 ± 18.96**
^{131}I-rituximab (IT, 150 μCi)	55.03 ± 9.94**
^{131}I-rituximab (IP, 150 μCi)	5.53 ± 17.72*
Control	56.01 ± 95.36

Compared with control cell group, * $P<0.05$ ** $P<0.01$.

Discussion

Currently, one inherent obstacle of radioimmunotherapy, suggested by many clinical results, is that radioimmunotherapy administered intravenously, does not generate a high therapeutic concentration of the radiolabelled antibodies in tumors[3-6]. One efficient approach used to circumvent this problem is intratumoral injection of the labeled monoclonal antibody[7-9]. In this experiment, we studied the distribution and antitumor activity of ^{131}I labeled Rituximab injected intratumorally or intraperitoneally in vivo in nude mice bearing Raji human Burkitt' s lymphoma xenografts, which provided some experimental evidence for the clinical applications of radioimmunotherapy.

CD20 is expressed on approximately 90% of Raji cells. ^{131}I-Rituximab, once injected intratumorally, can bind specific CD20 antigens, resulting in great regional radioactivity. In our experiment, the SPECT imaging results showed that the tumor %ID/g, and the cumulative absorbed dose of the radiolabelled antibodies in tumors were much more favorable in the ^{131}I-Rituximab IT group than in the ^{131}I-IgG IT group, which suggested that immunological binding, instead of retention of McAb in tumors, played a role in binding the ^{131}I-Rituximab with the tumor cells.

Similar experiments done previously on tumor-bearing mice often used intravenous or intraperitoneal routes of injection, which generally resulted in a similar biodistribution of the radiolabelled antibodies. Current challenges include[3-6] the labeled antibody being diluted by blood or neutralized by the free antigens in blood circulation, insufficient tumor penetration and nonspecific binding to other tissues. To overcome the above-mentioned unfavorable factors, intratumoral injection was employed in our experiment. Compared with intraperitoneal injection, intratumoral injection reduced the necessity of systematic exposure to the labeled antibody, while the labeled antibodies being bound, whose special radioactivity and immunoreactivity reached the peak, was optimal, resulting in the strongest cytotoxic effects.

In our experiment, the highest %ID/g in tumors was noticed at the moment of injection, and this was followed by a rapid decrease within 72 h and subsequently by a slow reduction. It was evident that binding the anti-CD20 monoclonal antibody to tumor cells was achieved in a short time. The cumulative absorbed dose of the radiolabelled antibodies in tumors in the IT group was 6.0- to 12.6-fold of that in the IP group, yet compared with intraperitoneal injection, intratumoral injection reduced %ID/g lower in non-tumors at each time point. Therefore intratumoral injection led to a favorable therapeutic effect and meanwhile reduced the toxicity and side effects induced by the nonspecific distribution of the radiolabeled antibodies.

The β-emitting ^{131}I is well known for its cytotoxic effects. When the mixture of ^{131}I and anti-CD20 monoclonal antibody was injected intratumorally, ^{131}I was unable to specifically target tumor tissue so that, in our experiment, the %ID/g in tumors was reduced from 192.4 at the moment of injection to 0.6 at 24 h after injection. The culmulative absorbed dose was not enough to kill tumors, which demonstrated that the labeling process of radionuclide played a key role in radioimmunotherapy.

The dose-rate effect of the radioimmunotherapy is generally accepted in clinical practice[10]. Although the relationship among dose-rate effect, tumor repair, and tumor growth rate is complex and beyond the scope of our present experiment, it calls for further studies, as suggested by our experimental results. The ^{131}I-rituximab injected intratumorally inhibited tumor growth in a dose-dependent manner, and the inhibition rate was less with low dose (75 μCi) injection but greater with high dose (150 μCi), whereas the difference was not significant ($P > 0.05$).

Although the ^{131}I-IgG injected intratumorally had certain inhibitive effects on the growth of Raji lymphoma within a short period, the inhibition rate was reduced to a very low level on the 24th day after injection, indicating that the nonspecific polyclonal antibody was not as effective as the specific monoclonal antibody in terms of tumor growth inhibition. This has been confirmed by many other experimental results done previously[11-15]. Because the CD20 expression on breast cancer MCF7 cells and lung cancer CD20 cells were negative, ^{131}I-Rituximab injected intratumorally had no inhibitive effects on the growth of MCF7 and A549 cell xenografts. Therefore monoclonal antibodies play an important role in radioimmunotherapy.

To conclude, intratumoral injection of the ^{131}I-Rituximab, as our experimental results suggested, resulted in the maximum uptake of the radiolabelled antibodies in tumors and in optimal antitumor activity. Due to the nature of systemic disease, lymphoma should be primarily treated using systematic therapy. To this point, our experimental results have built up a primary foundation for further exploring lymphoma treatment using systematic and regional radioimmunotherapy.

References

1 Tedder TF, Engel P. CD20: a regulator of cell-cycle progression of B lymphocytes. Immunol Today 1994; 15: 450–454.
2 Dillman LT. Radionuclide decay schemes and nuclear parameters for use in radiation dose estimation MIRD pamphlet. No.10, New York: Society of Nuclear Medicine 1975.
3 Patel S, Stein R, Ong GL, et al. Enhancement of tumor-to-nontumor localization ratios by hepatocyte-directed blood clearance of antibodies labeled with certain residualizing radiolabels. J Nucl Med 1999; 40: 1392–1401.
4 Press OW, Rasey J. Principles of radioimmunotherapy for hematologists and oncologists. Semin Oncol 2000; 27: 62–73.
5 Kinuya S, Li XF, Yokoyama K, et al. Intraperitoneal radioimmunotherapy in treating peritoneal carcinomatosis of colon cancer in mice compared with systemic radioimmunotherapy. Cancer Sci 2003; 94: 650–654.
6 Wider PR, Denardo GL, Denard SJ. Radioimmunotherapy recent results and future direction. J Clin Oncol 1996; 14: 1383–1400.
7 Kaminski MS, Estes J, Zasadny KR, et al. Radioimmunotherapy with iodine (131)I tositumomab for relapsed or refractory B-cell non-Hodgkin lymphoma: updated results and long-term follow-up of the University of Michigan experience. Blood 2000; 96: 1259–1266.
8 Vose JM, Wahl RL, Saleh M, et al. Multicenter phase II study of iodine-131 tositumomab for chemotherapy-relapsed/refractory low-grade and transformed low-grade B-cell non-Hodgkin's lymphomas. J Clin Oncol 2000; 18: 1316–1323.
9 Reddy LH, Murthy RS. Pharmacokinetics and biodistribution studies of Doxorubicin loaded poly (butyl cyanoacrylate) nanoparticles synthesized by two different techniques. Biomed Pap Med Fac Univ Palacky Olomouc Czech Repub 2004; 148: 161–166.
10 Dale RG. Dose-rate effects in targeted radiotherapy. Phys Med Biol 1996; 41: 1871–1884.
11 Vogel CA, Galmiche MC, Buchegger F. Radioimmunotherapy and fractionated radiotherapy of human colon cancer liver metastases in nude mice. Cancer Res 1997; 57: 447–453.
12 O'Donnell RT, DeNardo SJ, Yuan A, et al. Radioimmunotherapy with (111)In/(90)Y-2IT-BAD-m170 for metastatic prostate cancer. Clin Cancer Res 2001; 7: 1561–1568.
13 Yang XD, Jia XC, Jose RF, et al. Eradication of established tumors by a fully human monoclonal antibody to the epidermal growth factor receptor without concomitant chemotherapy. Cancer Res 1999; 59: 1236–1243.
14 Fani M, Vranjes S, Archimandritis SC, et al. Labeling of monoclonal antibodies with 153Sm for potential use in radioimmunotherapy. Appl Radiat Isot 2002; 57: 665–674.
15 de Jong GM, Boerman OC, Heskamp S, et al. Radioimmunotherapy prevents local recurrence of colonic cancer in an experimental model. Br J Surg 2009; 96: 314–321.